Gaseous *pvTx* Properties of Mixtures of Carbon Dioxide and Propane with the Burnett Isochoric Method

Xiao-Juan Feng, Qiang Liu, Meng-Xia Zhou, and Yuan-Yuan Duan*

Key Laboratory for Thermal Science and Power Engineering of MOE, Tsinghua University, Beijing, 100084, P. R. China

The gaseous *pvTx* properties of CO_2 (1, CAS No. 124-38-9) + propane (2, CAS No. 74-98-6) mixtures were measured using the Burnett-isochoric method with 225 data points obtained for temperatures from (320 to 400) K, pressures up to 7784 kPa, and densities up to 141 $kg\cdot m^{-3}$ at $x_1 = 0.5158$ and $x_1 = 0.8017$. Burnett measurements for argon (CAS No. 7440-37-1) were conducted at 319 K and for CO_2 at 343 K. The *pvT* properties and virial coefficients of argon and CO_2 agreed well with literature results when the effective cell constant for each fluid instead of that of the helium calibration was used in the density calculations. The temperature, pressure, density, and mole fraction uncertainties were estimated to be ± 5 mK, ± 300 Pa, ± 0.05 %, and ± 0.01 %, respectively. A truncated virial equation was used to correlate the experimental *pvTx* data of CO_2 + propane mixtures with root-mean-square deviations of ± 0.03 %. The second and third virial coefficients for the binary mixtures were also determined.

Introduction

Environmentally friendly working substances have succeeded in preventing the ozone layer from being destructed by anthropogenic chemicals, and they are also important in decelerating the climate change. Natural refrigerants such as hydrocarbons, carbon dioxide, and ammonia have attracted increasing attention because of their zero ozone-depletion potentials and low global-warming potentials.[1] However, the disadvantages of each pure natural refrigerant have restricted their wide applications. Mixtures are one option to provide useful refrigerants. Binary mixtures of carbon dioxide and propane are promising alternative refrigerants to replace R13 in low temperature cycles when the evaporator temperature is higher than 201 K,[2] and these mixtures can also be used as solvents to extract oil from seeds.[3,4]

Various *pvTx* measurements[5−9] and cross virial coefficient data[10−14] have been published for such mixtures for the liquid and/or gaseous phases since 1951. However, the published gaseous *pvTx* data for this mixture shows a maximum discrepancy larger than 2 %,[8] which is not precise enough to establish an equation of state. There are only 15 data points for the second cross virial coefficient for the limited temperature range from (273 to 333) K with an uncertainty larger than ± 5 $cm^3\cdot mol^{-1}$.[15] Thus, the Burnett isochoric method was used here to precisely measure the gaseous *pvTx* properties of CO_2 + propane mixtures for temperatures from (320 to 400) K and pressures up to 7784 kPa to provide more accurate *pvTx* data and virial coefficients over a larger temperature range. To validate the results for mixtures reliably, the experimental system was tested with pure CO_2 and argon.

Experimental System

Apparatus. The Burnett isochoric coupling method was used for the measurements. A diagram of the apparatus is shown in Figure 1. The system was rebuilt from a previous system with improved thermostatic baths, temperature measurement system, pressure measurement system, vacuum system, and data acquisition system as described by Feng et al.[16] The system has been used to accurately measure vapor pressures of fluorinated propanes.[17] The system used here was the same as that vapor pressure measurement system except for a new sensitive diaphragm pressure transducer with smaller random errors and zero drift.

The overall temperature uncertainty was estimated to be within ± 5 mK, including the ± 2 mK uncertainty of the platinum resistance thermometer, the ± 0.3 mK uncertainty of the thermometer bridge (model: MI 6242T), and the ± 3.4 mK stability and uniformity uncertainty of the thermostatic bath. The temperature was determined on the basis of the International Temperature Scale of 1990 (ITS-90). Before the experiments, the platinum resistance thermometers, the thermometer bridge, and the digital manometers were calibrated by the National Institute of Metrology (NIM), China.

The pressure measurement system, which could measure pressures from (0 to 10) MPa, included an absolute digital manometer (model: Yokogawa, MT 210, (0 to 130) kPa), two gauge pressure digital manometers (model: Yokogawa, MT 210, (0 to 3500) kPa; Ruska, 7050i, (0 to 10) MPa) and a sensitive diaphragm pressure transducer (model: Rosemount 3051S, (0 to 20) kPa). The pressure uncertainty was estimated to be less than ± 300 Pa including the uncertainty of the absolute digital manometer of ± 30 Pa from (0 to 130) kPa, the uncertainty of the gauge pressure digital manometer (MT210) of ± 80 Pa from (0 to 3500) kPa, the uncertainties of the Ruska manometer of ± 0.005 %, and the uncertainty of the differential pressure detector of less than ± 20 Pa.

A turbo-molecular pump (model: KYKY, FD 110) with an extreme vacuum of $1\cdot 10^{-6}$ Pa provided the vacuum for the experimental system.

The Burnett apparatus including the two cells was made of 1Cr18Ni9Ti stainless steel. The insides of the sample cell, B2, with a volume of 500 mL and the expansion cell, B1, with a volume of 200 mL were polished to reduce the physical

* To whom correspondence should be addressed. Tel.: +86-10-6279-6318. Fax: +86-10-6277-0209. E-mail: yyduan@tsinghua.edu.cn.

10.1021/je100148h
Published on Web 06/15/2010

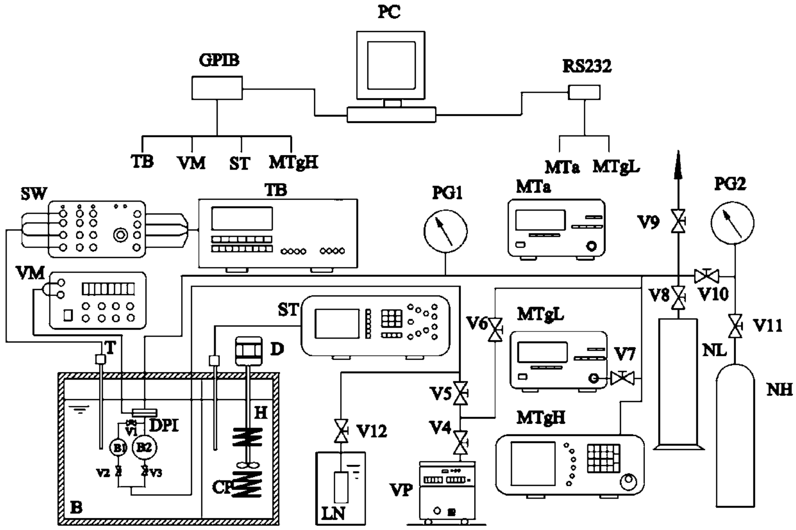

Figure 1. Burnett isochoric experimental apparatus: B, thermostatic bath; B1, expansion cell (200 mL); B2, sample cell (500 mL); CP, cooler; D, stirrer; DPI, differential pressure detector; H, heater; LN, liquid nitrogen; MTa, absolute pressure digital manometer; MTgL/MTgH, gauge pressure digital manometer for low and high pressures; NH, N_2 bottle; NL, pressure damper; PC, personal computer; PG1, PG2, pressure gauges; ST, HART 1590 super thermometer; SW, selector switch; T, platinum resistance thermometer; TB, MI 6242T thermometer bridge; V1 to V12, valves; VM, digital multimeter; VP, vacuum pump.

adsorption effects of experimental fluids onto the cell surfaces. Before the experiments, the two cells were rinsed with acetone and the experimental fluids to remove any residue from previous experiments. The valves in the Burnett system were changed in this work to reduce the microleakage.

A gas chromatograph (model: Shimadzu, GC 2014) with a thermal conductivity detector (TCD) and a 3 m × 3 mm Porapak-Q column was used to measure the sample purities and the mixture compositions. Ultrapure helium (99.999 %) was used as the carrier gas at a flow rate of 45 $mL \cdot min^{-1}$. The column temperatures were programmed for each fluid from (308 to 373) K. The oven and TCD temperatures were set to 373 K. After injection of the sample into the column, the effluence was analyzed for 20 min. The impurity evaluations were based on the GC area ratios.

Samples. Helium and argon samples with stated mole purities of 99.999 % were obtained from Air Products Corp. and Qianxi Corp., respectively. The CO_2 sample was obtained from Beiwen Gas Corp. with the stated mole purity of 99.995 %. The propane sample was obtained from Huayuan Gas Corp. with the stated mole purity of 99.95 %. Helium and argon were used without further purification. The CO_2 sample was also used without further purification except for being cooled in liquid nitrogen and evacuated by a vacuum pump to remove possible air impurities. The CO_2 sample impurities measured by the GC system were less than 0.005 %. The propane was purified from 99.93 % to 99.97 % (percentages are in terms of the area ratios of the GC measurements, approximate to mole fraction) based on the different boiling points of propane and the impurities.

Absolute deviations of measured vapor pressures of propane samples are shown in Figure 2. The reference vapor pressures of propane were calculated from Lemmon and Goodwin.[18] Several sets of representative accurate vapor pressures are also plotted in Figure 2. The vapor pressures of 99.93 % propane showed small positive deviations below 360 K but were (3 to 6) kPa higher than other data near the critical region. Vapor pressures of purified propane (99.97 %) of this work matched well with the measured results of McLinden[19] and Thomas and Harrison[20] and the calculated value of Lemmon et al.[21] Experimental vapor pressures from Kratzke[22] were lower than

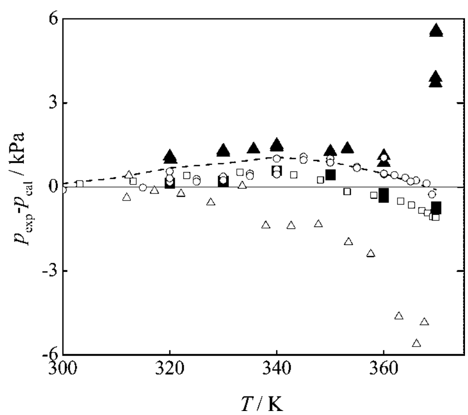

Figure 2. Absolute deviations of vapor pressures for propane: ■, purified sample, 99.97 %; ▲, sample before purification, 99.93 %; ○, McLinden;[19] □, Thomas and Harrison;[20] △, Kratzke;[22] ---, Lemmon et al.[21]

the other results perhaps due to the systematic errors and/or impurities in the samples. The deviations of vapor pressures of purified and unpurified propane correlated well with the GC analysis results that the propane contained impurities with higher boiling points such as ethane.

Great efforts were made for the mixture measurements to prepare the samples with accurate mole fractions. The masses of CO_2 and propane introduced into sample cell B2 were determined by measuring the weight changes of cylinders containing each component using an accurate electronic balance (model: Mettler Toledo, PR 1203) with a precision of ± 0.001 g. The cylinders were rinsed with the samples more than three times and evacuated to vacuum at a level lower than $5 \cdot 10^{-5}$ Pa. The mass of the cylinders was carefully measured to exclude systematic errors. Possible errors can occur due to (1) adsorption of water on the surface of the cylinders after cooling with liquid nitrogen, (2) microleakage of the cylinder valves and cylinders, one cylinder accidently having sand holes resulting in leakage, and (3) the position and direction of the cylinders on the balance. In this work, the masses were measured more than three times to obtain an accurate initial mole fraction for the mixtures. During each Burnett expansion procedure, the expansion valve V1 was open for more than 45 min with the thermostatic bath temperature controlled to maintain the constant mole fraction, and after measurement of each density, the samples in the expansion cell B1 were collected in a cooled, evacuated cylinder and then heated to room temperature and introduced into the GC system to measure the mole fraction. The uncertainty of the calculated mixture compositions was estimated to be less than ± 0.0001 mole fraction, and the GC results showed a stable mole fraction during the Burnett expansion procedures.

Experimental Procedure and Validation

The Burnett isochoric method developed by Burnett in 1963[23] is a traditional method for accurate $p\upsilon T(x)$ measurements. First, the temperature and pressure were measured on an isochoric line, and then the samples were expanded from the sample cell to expansion cell at the highest temperature to reduce the density. The isothermal expansion was repeated for several isochors to obtain temperatures and pressures for the whole measured region. The densities were calculated as:

$$\rho_i = \frac{p_i}{Z_i RT} = \frac{1}{N^i ART} \tag{1}$$

where ρ_i denotes the molar density, p_i is the pressure, $Z_i = p_i/\rho_i RT$ is the compressibility factor, R is the universal gas constant, T is the temperature, N is the cell constant, and i is the expansion number.

$$N \equiv \frac{V_1 + V_2}{V_2} \tag{2}$$

where V_1 is the volume of cell B1 and V_2 is the volume of cell B2.

A is the gas-filled constant:

$$\frac{1}{A} = \lim_{p_i \to 0} p_i N^i \tag{3}$$

Theoretically, the cell constant N is a function of only the experimental volumes of the cells and does not change with the experimental fluid. Since the two cells were made of the same stainless steel, our experience is that the cell constant was independent of temperature but a weak function of pressure:

$$N(p_{i-1}, p_i) = N_0 \frac{1 + mp_i}{1 + mp_{i-1}} \tag{4}$$

where m is a constant calculated from the mechanical properties of the material of the cells and $N_0 = \lim_{p_i \to 0} p_{i-1}/p_i$. Accurate cell constants are usually obtained using helium as the standard calibration gas in the Burnett method due to its small third virial coefficient and good linearity of p_{i-1}/p_i versus p_i.

The gas-filled constant A was fit from a least-squares program using experimental data for each experimental run.

The truncated virial equation, eq 5, is usually used to describe the gaseous $p\upsilon T(x)$ properties. The second and third virial coefficients B and C can also been determined from eq 5 by analysis of the $(Z - 1)/\rho$ versus ρ plot along an isotherm,

$$(Z - 1)/\rho = B + C\rho \tag{5}$$

The second method to calculate the densities is to use data along an isochore starting with the density at the highest temperature (400 K) determined from eq 1 for each Burnett expansion step combined with the calculated cell expansion characteristics for each temperature and pressure. The densities were calculated with both methods with differences within ± 0.05 %. The present densities from this work were calculated using the first method because the exact thermal expansion coefficient of the cell was unknown, and all of measured fluids were nonpolar with negligible adsorption on the cell surfaces.

Table 1. Helium Calibration Results

T	pressure range		B	B^{15}	B^{24}
K	kPa	N_0	$cm^3 \cdot mol^{-1}$	$cm^3 \cdot mol^{-1}$	$cm^3 \cdot mol^{-1}$
318.165	138 to 6676	1.378010 ± 0.00002	11.40 ± 0.1	11.67 ± 0.3	11.30
343.127	563 to 7534	1.378092 ± 0.00005	11.21 ± 0.1	11.55 ± 0.3	11.18

The temperature and pressure data were recorded by a data acquisition system. During the high-pressure measurements, the operation should be done extremely carefully because dozens of openings and closings of the expansion valve V1 can cause abrasions of the needle inside the valve that may result in microleakage. As expansion cell B1 was evacuated, the pressures in sample cell B2 were also recorded to detect leakage.

Helium Calibration. Table 1 lists the detailed results of helium calibration before and after measurements of the mixtures at temperatures of (318 and 343) K. The second virial coefficients agreed well with the Dymond[15] correlation and REFPROP 8.0[24] as shown in Table 1 and Figure 3. The cell constant N_0 slightly shifted due to random errors or the abrasion of the needle in the expansion valve V1, resulting in small shifts of the cell volumes. In $p\upsilon T(x)$ measurements using the Burnett isochoric method, the experimental system uncertainties and the data reduction procedure are both important to obtain accurate data. Especially when $p\upsilon T(x)$ data are used to calculate the virial coefficients, the systematic and random errors may accumulate at low pressures resulting in large uncertainties of virial coefficients. The agreement of the virial coefficients for helium validates that temperature and pressure measurements as well as the data reduction procedure are reliable.

CO_2. After the measurements for mixtures of CO_2 (1) + propane (2) ($x_1 = 0.5158$), the gaseous $p\upsilon T$ properties of pure CO_2 were measured at a supercritical temperature of 343.13 K to validate the experimental system and the data reduction program for other fluids. The $(Z - 1)/\rho$ versus ρ plot departed from linear values with an obvious downward trend at the low densities plotted in Figure 4. The systematic errors with $(Z - 1)/\rho$ versus ρ plot for CO_2 look like the "adsorption effect".[25] However, nonpolar, supercritical CO_2 should have negligible adsorption on the polished stainless steel surfaces. The CO_2 samples were tested on the GC system before and after the Burnett expansions with no impurities found by the GC analysis. Since the temperature and pressure measurement systems and the data reduction program to obtain the gas-filled constant A had been tested with helium, the possible reasons for these discrepancies depend on the samples and cell constant N_0. The

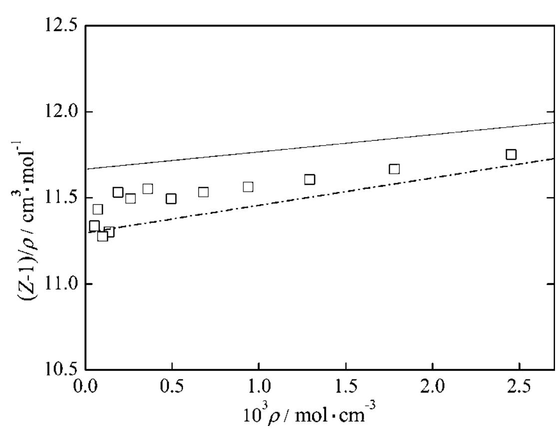

Figure 3. $(Z - 1)/\rho$ vs ρ for helium at 318.165 K: □, experimental results; ----, REFPROP 8.0;[24] —, correlation results from Dymond et al.[15]

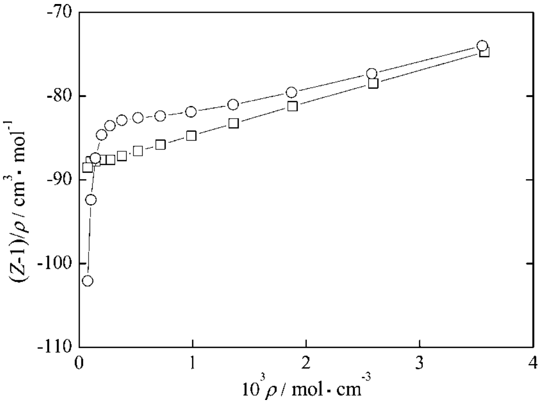

Figure 4. $(Z - 1)/\rho$ vs ρ for CO_2 at 343.132 K: □, $U_0 = 1.378854$; ○, $N_0 = 1.378092$.

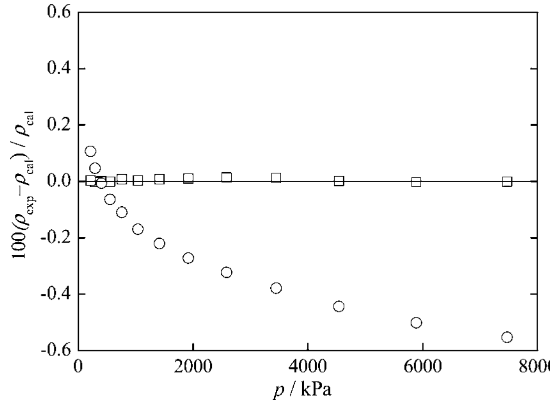

Figure 5. Relative density deviations for CO_2 compared to results from Span and Wagner:[27] □, $U_0 = 1.378854$; ○, $N_0 = 1.378092$.

Table 2. Experimental $p\upsilon T$ Data for CO_2

T	p	ρ/kg·m^{-3}	ρ/kg·m^{-3}
K	kPa	$U_0 = 1.378854$	$N_0 = 1.378092$
343.133	7469.20	157.178	156.310
343.132	5888.24	114.017	113.448
343.131	4543.03	82.704	82.336
343.134	3447.34	59.988	59.754
343.131	2584.25	43.511	43.365
343.133	1919.84	31.558	31.469
343.133	1416.95	22.889	22.837
343.133	1040.75	16.600	16.572
343.128	761.77	12.040	12.026
343.133	556.21	8.732	8.727
343.130	405.34	6.333	6.333
343.134	295.01	4.593	4.595
343.131	214.49	3.331	3.335

Table 3. Second and Third Virial Coefficients for CO_2 at 343.132 K

	B	C
	cm^3·mol^{-1}	cm^6·mol^{-2}
$U_0 = 1.378854$	-88.55 ± 0.1	3869 ± 50
$N_0 = 1.378092$ (10 points)	-84.55 ± 0.1	2861 ± 50
Dymond et al. (correlation results)[15]	-88.8 ± 0.3	3821 ± 120
Span and Wagner[27]	-88.5	3997

Table 4. Experimental $p\upsilon T$ Data for Argon

T	p	ρ/kg·m^{-3}	ρ/kg·m^{-3}
K	kPa	$U_0 = 1.378205$	$N_0 = 1.378092$
318.755	7231.46	111.747	111.681
318.755	5275.06	81.092	81.051
318.751	3845.47	58.845	58.820
318.751	2800.67	42.700	42.685
318.759	2038.22	30.983	30.975
318.758	1482.26	22.482	22.477
318.755	1077.30	16.313	16.311
318.755	782.65	11.836	11.836
318.751	568.39	8.589	8.589
318.750	412.69	6.232	6.233
318.752	299.59	4.522	4.523
318.752	217.45	3.281	3.282
318.756	157.82	2.381	2.382

calculated cell constant for CO_2 should be the same as the apparatus constant N_0. However, the cell constant for CO_2 (1.378854 ± 0.00006) was 0.06 % larger than the helium calibration results (first run: 1.378010 ± 0.00002; second run: 1.378092 ± 0.00005).

Gupta and Eubank[26] faced similar problems and concluded that the cell constant changed for different fluids because "the valve packing were made of Teflon impregnated with graphite and its pores could swell in the presence of a solvent". The valve packing in this work was also made of Teflon impregnated with graphite, so the effective cell volume changed with different fluids.

Thus, the isotherm cell constant, U_0, for each fluid was used instead of the helium calibration results, N_0,

$$U_0 = \lim_{p_i \to 0} \frac{p_{i-1}}{p_i} \tag{6}$$

The densities calculated using $U_0 = 1.378854$ and $N_0 = 1.378092$ are listed in Table 2. The densities with $U_0 = 1.378854$ matched well with Span and Wagner's[27] calculated results with an average relative deviation of $\pm$ 0.005 %, while these using N_0 had large systematic deviations of -0.6 % at high pressures and 0.1 % at low pressures as shown in Figure 5. The second and third virial coefficients also agreed well with those of Dymond et al.[15] and Span and Wagner[27] listed in Table 3. The $(Z - 1)/\rho$ versus ρ plot was much straighter at low densities when the cell constant U_0 for CO_2 was used as shown in Figure 4 since the systematic density errors with $N_0 = 1.378092$ at low pressures are magnified when calculating $(Z - 1)/\rho$ and the virial coefficients.

When the "effective" cell constant U_0 was used in the data reduction procedure, the densities and virial coefficients matched better with published data. This conclusion was then validated using the Burnett measurement for argon after the experiments for mixture 2 ($x_1 = 0.8017$).

Argon. The Burnett $p\upsilon T$ properties of argon were measured at 318.75 K from (158 to 7231) kPa. The cell constant U_0 for argon was estimated to be 1.378205 ± 0.00004. The densities calculated with the cell constants U_0 and N_0 with results are shown in Table 4 and Figure 6. The densities with $U_0 = 1.378205$ matched well with results from Tegeler et al.[28] with an average relative deviation of $\pm$ 0.002 %. The second and third virial coefficients listed in Table 5 also show that when the cell constant U_0 is used, it provides reliable results. The plot of $(Z - 1)/\rho$ versus ρ in Figure 7 shows a similar trend as with the CO_2 which validates that the effective cell constant U_0 should be used for each fluid instead of the helium calibration results.

In summary, helium was used as the calibration gas to determine the cell constant N_0 before and after the mixture measurements. The reliability of the experimental system and data reduction procedure was then validated using gaseous $p\upsilon T$ measurements for pure CO_2 carefully after the measurements with mixture 1. Measurements with gaseous argon were used to further verify the conclusions after the measurements with mixture 2. The results indicate that the valve packing swelled

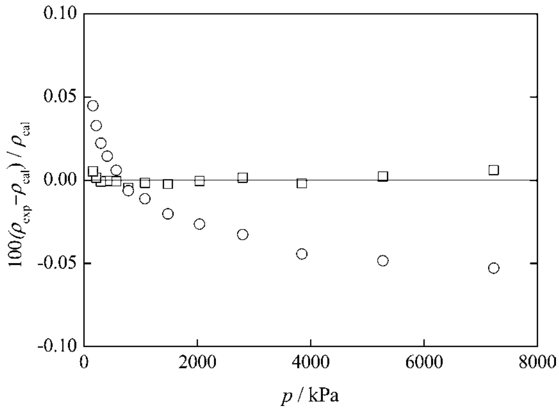

Figure 6. Relative density deviations for argon compared to results from Tegeler et al.:[28] □, $U_0 = 1.378205$; ○, $N_0 = 1.378092$.

Table 5. Second and Third Virial Coefficients for Argon at 318.754 K

	B	C
	$cm^3 \cdot mol^{-1}$	$cm^6 \cdot mol^{-2}$
$U_0 = 1.378205$	−11.63 ± 0.1	1006 ± 40
$N_0 = 1.378092$ (7 data points)	−11.30 ± 0.1	965 ± 40
Dymond et al. (correlation results)[15]	−11.91 ± 0.3	1088 ± 80
Tegeler et al.[28]	−11.51	1008

different amounts for different fluids and released in the vacuum resulting in reversible changes of the cell volume.

Results and Discussion for CO_2 + Propane

A total of 225 $p\upsilon Tx$ data points for the binary CO_2 (1) + propane (2) mixture were obtained in the gaseous phase with temperatures from (320 to 400) K, pressures up to 7784 kPa, and two mixture compositions of $x_1 = 0.5158$ ($w_1 = 0.5153$) and $x_1 = 0.8017$ ($w_1 = 0.8014$). The temperature (T/K), pressure (p/kPa), density (ρ/kg·m^{-3}), compressibility factor (Z), and CO_2 mole fraction (x_1) data are listed in Table 6. The effective cell constant U_0 for mixture 1 ($x_1 = 0.5158$) was estimated to be 1.379601 and for mixture 2 ($x_1 = 0.8017$) was 1.379070 for calculating the densities and compressibility factor. The 0.04 % difference between the two effective cell constants comes from the different solubility of propane and CO_2 in the valve packing.

The relative uncertainties for the density and compressibility factor are ± 0.05 % and ± 0.06 % at a 95 % confidence level. Figure 8 show the $p\upsilon Tx$ data with the propane vapor pressures calculated from Lemmon et al.[21] Figure 9 shows the $(Z - 1)/\rho$ versus ρ plot for mixture 2 ($x_1 = 0.8017$) when different cell constants were used to calculate the results which also show that the effective cell constant U_0 should be used. The $(Z - 1)/\rho$ versus ρ plot for the mixture also proved that this trend was not caused by the adsorption effect between gases and surfaces of experimental cells because the $(Z - 1)/\rho$ versus ρ plot showed similar trends at different temperatures, while the adsorption effect was a strong function of the temperature.

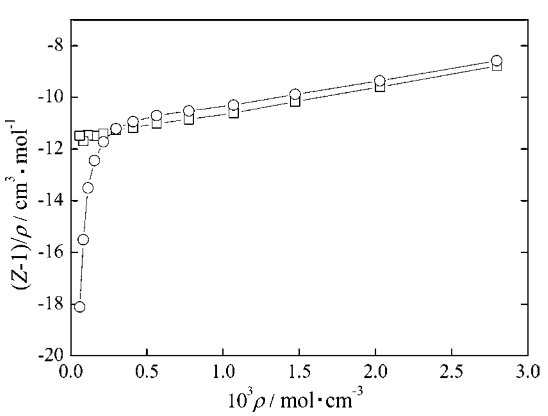

Figure 7. $(Z - 1)/\rho$ vs ρ for argon at 318.754 K: □, $U_0 = 1.378205$; ○, $N_0 = 1.378092$.

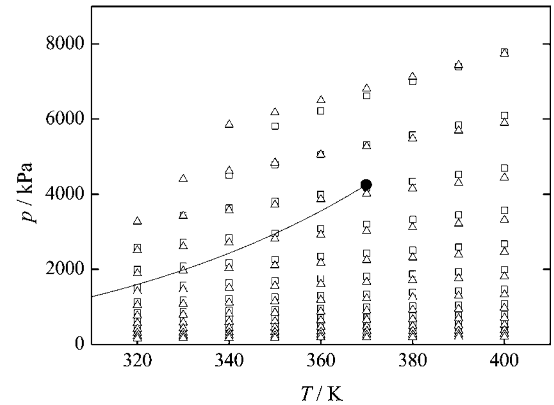

Figure 8. Distribution of experimental CO_2 (1) + propane (2) data: □, $x_1 = 0.5158$; △, $x_1 = 0.8017$; ●, critical point of propane; —, vapor pressures for propane.

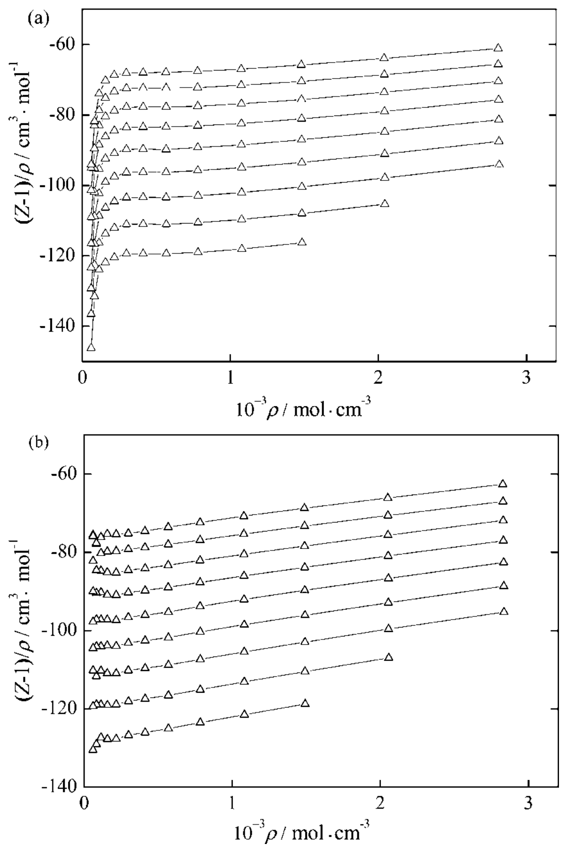

Figure 9. $(Z - 1)/\rho$ vs ρ for CO_2 (1) + propane (2) ($x_1 = 0.8017$): (a) $N_0 = 1.378092$; (b) $U_0 = 1.379070$.

A truncated virial equation of state for the CO_2 (1) + propane (2) system was developed by fitting the data listed in Table 6. The equation was based on the following functional form:

$$Z = \frac{p}{\rho RT} = 1 + B_m\rho + C_m\rho^2 \qquad (7)$$

Table 6. Experimental $pvTx$ Data for the CO_2 (1) + Propane (2) Mixtures

T/K	p/kPa	ρ/kg·m^{-3}	Z	x_1	T/K	p/kPa	ρ/kg·m^{-3}	Z	x_1
400.028	7784.16	140.912	0.73164	0.5158	400.037	4441.75	65.486	0.89783	0.8017
400.026	6095.48	102.176	0.79013	0.5158	400.036	3314.32	47.495	0.92370	0.8017
400.035	4696.70	74.081	0.83968	0.5158	400.034	2454.95	34.445	0.94341	0.8017
400.034	3565.28	53.710	0.87917	0.5158	400.032	1808.37	24.980	0.95826	0.8017
400.042	2676.02	38.937	0.91022	0.5158	400.029	1326.55	18.115	0.96933	0.8017
400.035	1989.48	28.228	0.93346	0.5158	400.018	970.17	13.137	0.97758	0.8017
400.026	1468.73	20.463	0.95062	0.5158	400.033	707.92	9.526	0.98369	0.8017
400.034	1079.54	14.834	0.96388	0.5158	400.028	515.70	6.908	0.98818	0.8017
400.029	790.53	10.753	0.97372	0.5158	400.029	375.15	5.009	0.99134	0.8017
400.030	577.33	7.794	0.98102	0.5158	400.034	272.65	3.632	0.99360	0.8017
400.037	420.82	5.650	0.98648	0.5158	400.035	198.07	2.634	0.99546	0.8017
400.044	306.29	4.095	0.99053	0.5158	390.029	7432.39	124.497	0.81051	0.8017
400.035	222.65	2.968	0.99342	0.5158	390.032	5688.28	90.301	0.85521	0.8017
390.027	7399.00	141.004	0.71281	0.5158	390.029	4298.50	65.497	0.89101	0.8017
390.022	5838.53	102.241	0.77574	0.5158	390.030	3214.68	47.503	0.91877	0.8017
390.027	4522.90	74.128	0.82883	0.5158	390.025	2384.93	34.451	0.93987	0.8017
390.025	3446.26	53.743	0.87108	0.5158	390.033	1758.82	24.983	0.95577	0.8017
390.033	2593.45	38.961	0.90421	0.5158	390.037	1291.27	18.117	0.96761	0.8017
390.029	1931.69	28.245	0.92903	0.5158	390.028	944.86	13.139	0.97637	0.8017
390.034	1427.95	20.475	0.94736	0.5158	390.029	689.66	9.528	0.98276	0.8017
390.029	1050.49	14.843	0.96143	0.5158	390.027	502.51	6.909	0.98748	0.8017
390.034	769.82	10.759	0.97194	0.5158	390.033	365.64	5.010	0.99087	0.8017
390.036	562.52	7.799	0.97977	0.5158	390.029	265.87	3.633	0.99358	0.8017
390.033	410.13	5.653	0.98549	0.5158	390.030	193.15	2.634	0.99548	0.8017
390.038	298.57	4.098	0.98973	0.5158	380.019	7122.68	124.564	0.79677	0.8017
390.028	217.06	2.970	0.99273	0.5158	380.024	5478.48	90.348	0.84492	0.8017
380.026	7010.29	141.070	0.69281	0.5158	380.021	4154.26	65.530	0.88335	0.8017
380.020	5579.29	102.287	0.76047	0.5158	380.021	3114.53	47.526	0.91314	0.8017
380.017	4347.62	74.161	0.81733	0.5158	380.026	2314.67	34.467	0.93575	0.8017
380.025	3326.52	53.766	0.86258	0.5158	380.021	1709.04	24.996	0.95272	0.8017
380.026	2510.44	38.978	0.89793	0.5158	380.023	1255.86	18.126	0.96539	0.8017
380.020	1873.61	28.257	0.92443	0.5158	380.022	919.55	13.145	0.97476	0.8017
380.021	1386.94	20.484	0.94399	0.5158	380.025	671.46	9.532	0.98155	0.8017
380.026	1021.40	14.849	0.95902	0.5158	380.026	489.43	6.912	0.98664	0.8017
380.033	749.01	10.763	0.97018	0.5158	380.029	356.25	5.012	0.99036	0.8017
380.032	547.58	7.802	0.97847	0.5158	380.025	259.02	3.635	0.99302	0.8017
380.025	399.41	5.656	0.98459	0.5158	380.025	188.21	2.635	0.99508	0.8017
380.039	290.81	4.099	0.98900	0.5158	370.021	6810.40	124.620	0.78207	0.8017
380.039	211.45	2.971	0.99212	0.5158	370.009	5266.97	90.391	0.83389	0.8017
370.020	6617.03	141.135	0.67132	0.5158	370.020	4009.41	65.558	0.87522	0.8017
370.017	5317.21	102.331	0.74401	0.5158	370.011	3013.86	47.548	0.90712	0.8017
370.016	4171.02	74.192	0.80499	0.5158	370.011	2244.05	34.483	0.93133	0.8017
370.018	3205.97	53.788	0.85345	0.5158	370.004	1659.14	25.007	0.94950	0.8017
370.020	2426.93	38.994	0.89117	0.5158	370.013	1220.32	18.134	0.96303	0.8017
370.016	1815.28	28.268	0.91949	0.5158	370.015	894.13	13.150	0.97304	0.8017
370.016	1345.82	20.492	0.94039	0.5158	370.013	653.23	9.536	0.98031	0.8017
370.020	992.19	14.855	0.95640	0.5158	370.011	476.31	6.915	0.98573	0.8017
370.028	728.17	10.768	0.96830	0.5158	370.022	346.79	5.014	0.98973	0.8017
370.027	532.61	7.805	0.97706	0.5158	370.016	252.19	3.636	0.99254	0.8017
370.023	388.65	5.658	0.98360	0.5158	370.018	183.24	2.637	0.99461	0.8017
370.023	283.04	4.101	0.98819	0.5158	360.023	6494.96	124.685	0.76616	0.8017
370.021	205.87	2.973	0.99167	0.5158	360.014	5054.02	90.435	0.82198	0.8017
360.011	6218.19	141.203	0.64809	0.5158	360.016	3863.46	65.591	0.86635	0.8017
360.011	5051.96	102.377	0.72622	0.5158	360.010	2912.64	47.571	0.90057	0.8017
360.011	3992.60	74.224	0.79163	0.5158	360.010	2173.16	34.499	0.92651	0.8017
360.013	3084.26	53.811	0.84351	0.5158	360.006	1608.88	25.019	0.94586	0.8017
360.015	2342.90	39.010	0.88386	0.5158	360.010	1184.71	18.143	0.96043	0.8017
360.014	1756.62	28.280	0.91413	0.5158	360.016	868.69	13.157	0.97115	0.8017
360.009	1304.50	20.501	0.93647	0.5158	360.016	634.97	9.541	0.97891	0.8017
360.011	962.87	14.861	0.95355	0.5158	360.016	463.19	6.918	0.98473	0.8017
360.006	707.21	10.772	0.96618	0.5158	360.022	337.31	5.017	0.98893	0.8017
360.012	517.62	7.809	0.97556	0.5158	360.019	245.35	3.638	0.99197	0.8017
360.015	377.87	5.660	0.98250	0.5158	360.016	178.29	2.638	0.99415	0.8017
360.008	275.27	4.103	0.98739	0.5158	350.018	6175.26	124.740	0.74894	0.8017
360.015	200.24	2.974	0.99096	0.5158	350.012	4838.83	90.473	0.80914	0.8017
350.010	5812.83	141.262	0.62289	0.5158	350.013	3716.34	65.618	0.85683	0.8017
350.010	4782.86	102.417	0.70691	0.5158	350.011	2810.84	47.589	0.89357	0.8017
350.009	3811.99	74.253	0.77712	0.5158	350.007	2101.90	34.513	0.92138	0.8017
350.012	2961.46	53.831	0.83276	0.5158	350.011	1558.64	25.028	0.94214	0.8017
350.014	2258.25	39.024	0.87595	0.5158	350.015	1148.99	18.150	0.95772	0.8017
350.013	1697.65	28.290	0.90837	0.5158	350.012	843.17	13.162	0.96917	0.8017
350.009	1263.00	20.508	0.93226	0.5158	350.009	616.66	9.544	0.97747	0.8017
350.010	933.45	14.866	0.95050	0.5158	350.020	450.01	6.921	0.98369	0.8017
350.008	686.24	10.776	0.96398	0.5158	350.017	327.80	5.019	0.98814	0.8017
350.009	502.56	7.811	0.97391	0.5158	350.020	238.49	3.639	0.99140	0.8017
350.013	367.05	5.662	0.98128	0.5158	350.011	173.33	2.639	0.99374	0.8017
350.011	267.49	4.104	0.98655	0.5158	340.010	5849.82	124.787	0.73008	0.8017
350.014	194.63	2.975	0.99034	0.5158	340.005	4621.28	90.506	0.79522	0.8017
340.008	4508.97	102.472	0.68566	0.5158	339.995	3567.86	65.643	0.84651	0.8017
340.012	3628.80	74.290	0.76114	0.5158	340.001	2708.23	47.606	0.88599	0.8017
340.009	2837.32	53.858	0.82090	0.5158	339.996	2030.23	34.525	0.91584	0.8017
340.015	2172.91	39.044	0.86721	0.5158	339.990	1508.12	25.038	0.93812	0.8017
340.015	1638.30	28.304	0.90195	0.5158	340.006	1113.10	18.156	0.95480	0.8017
340.008	1221.28	20.518	0.92752	0.5158	339.987	817.54	13.167	0.96705	0.8017

Table 6. Continued

T/K	p/kPa	ρ/kg·m^{-3}	Z	x_1	T/K	p/kPa	ρ/kg·m^{-3}	Z	x_1
340.012	903.91	14.873	0.94702	0.5158	339.990	598.29	9.548	0.97595	0.8017
340.010	665.18	10.781	0.96141	0.5158	340.002	436.79	6.923	0.98255	0.8017
340.007	487.50	7.815	0.97202	0.5158	340.013	318.30	5.020	0.98742	0.8017
340.016	356.19	5.665	0.97978	0.5158	340.003	231.59	3.641	0.99077	0.8017
340.009	259.67	4.106	0.98542	0.5158	340.008	168.38	2.640	0.99340	0.8017
340.013	189.01	2.976	0.98956	0.5158	329.999	4401.15	90.545	0.77997	0.8017
330.011	3442.62	74.321	0.74366	0.5158	329.991	3418.11	65.670	0.83522	0.8017
330.014	2711.71	53.880	0.80801	0.5158	329.999	2604.89	47.625	0.87766	0.8017
330.014	2086.76	39.059	0.85771	0.5158	330.001	1958.15	34.538	0.90975	0.8017
330.010	1578.47	28.315	0.89498	0.5158	329.987	1457.41	25.048	0.93369	0.8017
330.009	1179.41	20.526	0.92249	0.5158	330.006	1077.12	18.163	0.95157	0.8017
330.008	874.20	14.879	0.94328	0.5158	329.985	791.85	13.172	0.96468	0.8017
330.006	644.04	10.786	0.95869	0.5158	329.983	579.89	9.552	0.97422	0.8017
330.008	472.35	7.818	0.96999	0.5158	329.997	423.55	6.926	0.98128	0.8017
330.010	345.31	5.667	0.97826	0.5158	330.003	308.75	5.022	0.98644	0.8017
330.010	251.86	4.108	0.98436	0.5158	330.009	224.73	3.642	0.99017	0.8017
330.011	183.36	2.977	0.98871	0.5158	330.010	163.40	2.641	0.99284	0.8017
320.009	2584.00	53.913	0.79354	0.5158	320.002	3266.52	65.693	0.82281	0.8017
320.008	1999.59	39.083	0.84707	0.5158	320.003	2500.61	47.642	0.86853	0.8017
320.008	1518.12	28.332	0.88714	0.5158	320.001	1885.55	34.551	0.90306	0.8017
320.000	1137.15	20.539	0.91670	0.5158	319.998	1406.42	25.056	0.92884	0.8017
320.007	844.37	14.888	0.93902	0.5158	319.999	1040.92	18.170	0.94799	0.8017
320.009	622.82	10.792	0.95552	0.5158	319.992	766.06	13.176	0.96208	0.8017
320.007	457.20	7.823	0.96766	0.5158	320.001	561.41	9.555	0.97230	0.8017
320.007	334.43	5.670	0.97647	0.5158	319.999	410.29	6.929	0.97990	0.8017
320.010	244.02	4.110	0.98293	0.5158	320.013	299.21	5.024	0.98548	0.8017
320.012	177.71	2.979	0.98760	0.5158	320.011	217.81	3.643	0.98933	0.8017
400.029	7739.41	124.476	0.82303	0.8017	320.008	158.39	2.642	0.99217	0.8017
400.040	5896.58	90.285	0.86450	0.8017					

Table 7. Numerical Constants in Equations 10 and 11 for the CO_2 (1) + Propane (2) Mixtures

ij	$10^{-3}\,B_{0,ij}$	$10^{-3}\,B_{1,ij}$	$10^{-3}\,B_{2,ij}$	$10^{-3}\,B_{3,ij}$	$10^{-3}\,B_{4,ij}$	$10^{-3}\,B_{5,ij}$
	cm^3·mol^{-1}					
11	$5.455230 \cdot 10^{-2}$	$-1.131138 \cdot 10^{-1}$	$-2.429052 \cdot 10^{-2}$	$-3.278418 \cdot 10^{-2}$	$-1.929567 \cdot 10^{-3}$	$5.459091 \cdot 10^{-5}$
22	$1.851771 \cdot 10^{-1}$	$-5.001604 \cdot 10^{-1}$	$2.548089 \cdot 10^{-1}$	$-1.902483 \cdot 10^{-1}$	$5.253111 \cdot 10^{-3}$	$-5.911886 \cdot 10^{-4}$
12	$8.441618 \cdot 10^{0}$	$-3.548947 \cdot 10^{1}$	$5.279077 \cdot 10^{1}$	$-2.885843 \cdot 10^{1}$	$3.842602 \cdot 10^{0}$	$-8.639504 \cdot 10^{-1}$

ijk	$10^{-6}\,C_{0,ijk}$	$10^{-6}\,C_{1,ijk}$	$10^{-6}\,C_{2,ijk}$	$10^{-6}\,C_{4,ijk}$
	cm^6·mol^{-2}			
111	$7.706055 \cdot 10^{-2}$	$-2.219376 \cdot 10^{-1}$	$1.826413 \cdot 10^{-1}$	$-3.309323 \cdot 10^{-2}$
222	$1.381833 \cdot 10^{0}$	$-3.789965 \cdot 10^{0}$	$2.942843 \cdot 10^{0}$	$-5.143281 \cdot 10^{-1}$
112	$-3.746196 \cdot 10^{0}$	$1.064143 \cdot 10^{0}$	$-8.498415 \cdot 10^{0}$	$1.610709 \cdot 10^{0}$
122	$1.117382 \cdot 10^{0}$	$-2.940546 \cdot 10^{0}$	$2.169924 \cdot 10^{0}$	$-3.334814 \cdot 10^{-1}$

where B_m and C_m denote the second and third mixture virial coefficients given by:

$$B_m = \sum_i^2 \sum_j^2 x_i x_j B_{ij} \tag{8}$$

$$C_m = \sum_i^2 \sum_j^2 \sum_k^2 x_i x_j x_k C_{ijk} \tag{9}$$

Note that if $i = j = k$, B_{ij} and C_{ijk} correspond to the virial coefficients for the pure components. The virial coefficients B_{11}, C_{111}, B_{22}, and C_{222} of the pure CO_2 and propane were calculated from equations of Span and Wagner[27] and Lemmon et al.[21] with temperatures from (220 to 450) K. Both B_{ij} and C_{ijk} were expressed as functions of the reduced temperature $T_{r,ij(k)} = T/T_{c,ij(k)}$ as:

$$B_{ij} = B_{0,ij} + B_{1,ij}T_{r,ij}^{-1} + B_{2,ij}T_{r,ij}^{-2} + B_{3,ij}T_{r,ij}^{-3} + B_{4,ij}T_{r,ij}^{-6} + B_{5,ij}T_{r,ij}^{-8} \tag{10}$$

$$C_{ijk} = C_{0,ijk} + C_{1,ijk}T_{r,ijk}^{-0.5} + C_{2,ijk}T_{r,ijk}^{-1} + C_{3,ijk}T_{r,ijk}^{-2} \tag{11}$$

The characteristic temperature, $T_{c,ij(k)}$, was defined for the cross second and third virial coefficients of the mixture as:

$$T_{c,ij} = \sqrt{T_{c,i}T_{c,j}} \tag{12}$$

$$T_{c,ijk} = \sqrt[3]{T_{c,i}T_{c,j}T_{c,k}}$$

The critical temperature of CO_2 is 304.128 K,[29] and that of propane is 369.89 K.[21] The coefficients in eqs 10 and 11 for the CO_2 + propane mixtures are listed in Table 7.

Figure 10 shows the relative pressure deviations of the experimental data from eq 7. Thus, the data can be well-represented by the truncated virial equation with a root-mean-square (rms) deviation of 0.028 % over the entire range. The deviations of the density measurements from the present virial EOS are also shown in Figure 11. The detailed maximum and rms deviations are listed in Table 8.

The published $pvTx$ data from Reamer et al.,[5] Niesen and Rainwater,[6] de la Cruz de Dios et al.,[8] and Blanco et al.[9] with temperatures from (278 to 511) K are compared to eq 7 with the relative pressure and density deviations shown in Figures 12 and 13. The mole fractions of CO_2 for the published experimental data varied from (0 to 1). The deviations of the published data show much larger random errors than the data from this work. The maximum relative pressure deviation of the experimental data from Reamer et al.[5] is 1.0 % with CO_2 mole fractions of 0.7936, 0.5884, and 0.4017 at pressures below 5000 kPa. The experimental pressures from Reamer et al.[5] are

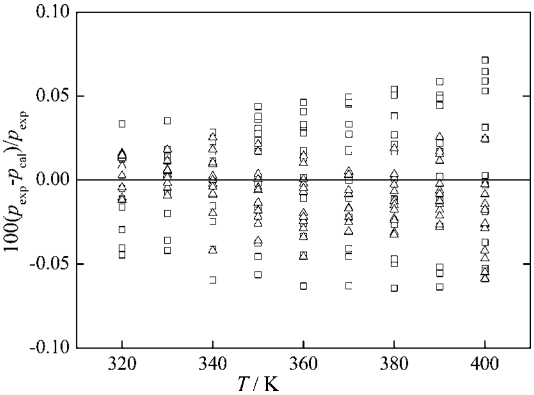

Figure 10. Pressure deviations of experimental $pvTx$ data from eq 7 for CO_2 (1) + propane (2) mixtures: □, $x_1 = 0.5158$; △, $x_1 = 0.8017$.

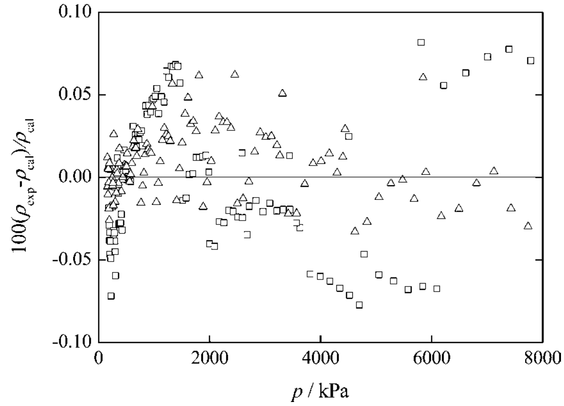

Figure 11. Density deviations of experimental $pvTx$ data from eq 7 for CO_2 (1) + propane (2) mixtures: □, $x_1 = 0.5158$; △, $x_1 = 0.8017$.

Table 8. Deviations of the Present $pvTx$ Data from Equation 7 for CO_2 (1) + Propane (2) Mixtures[a]

$100\cdot\delta_{max}(p)$	$100\cdot\delta_{rms}(p)$	$100\cdot\delta_{max}(\rho)$	$100\cdot\delta_{rms}(\rho)$
0.071	0.028	0.082	0.033

[a]

$$\delta_{max}(p) = \max(p_{i,exp}/p_{i,cal} - 1)$$

$$\delta_{rms}(p) = \sqrt{\sum_{i=1}^{n}(p_{i,exp}/p_{i,cal} - 1)^2/(n - 1)}$$

$$\delta_{max}(\rho) = \max(\rho_{i,exp}/\rho_{i,cal} - 1)$$

$$\delta_{rms}(\rho) = \sqrt{\sum_{i=1}^{n}(\rho_{i,exp}/\rho_{i,cal} - 1)^2/(n - 1)}$$

lower than eq 7 at $x_1 = 0.1962$ from (310 to 510) K. Note that eq 7 was correlated from present $pvTx$ data at temperatures from (320 to 400) K; nevertheless eq 7 can represent experimental data well at temperatures up to 450 K. At temperatures above 450 K, the experimental pressures from Reamer et al.[5] show increasing systematic discrepancies. The maximum densities deviation of the experimental data from Niesen and Rainwater[6] is 1.0 % at pressures lower than 4000 kPa with larger deviations at higher pressures. Most of the experimental data from de la Cruz de Dios et al.[8] show good agreement with eq 7 except at atmospheric pressure because de la Cruz de Dios et al.[8] measured the properties at high pressures up to 70 MPa with a pressure uncertainty of ± 1.3 kPa. Blanco et al.[9] measured the densities of CO_2 + propane at 308.15 K with larger random errors than the other data. The pressure and densities show larger

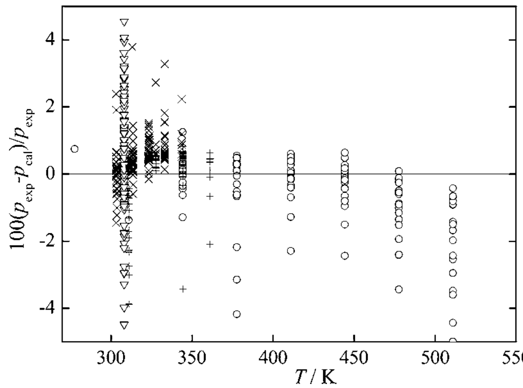

Figure 12. Pressure deviations of experimental $pvTx$ data from eq 7 for CO_2 (1) + propane (2) mixtures: ○, Reamer et al.;[5] +, Niesen and Rainwater;[6] ×, de la Cruz de Dios et al.;[8] △, Blanco et al.[9]

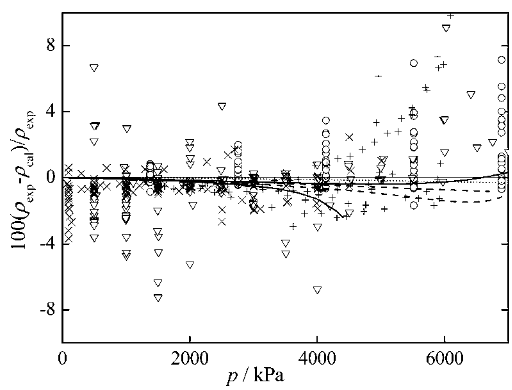

Figure 13. Density deviations of experimental $pvTx$ data from eq 7 for CO_2 (1) + propane (2) mixtures: ○, Reamer et al.;[5] +, Niesen and Rainwater;[6] ×, de la Cruz de Dios et al.;[8] ▽, Blanco et al.;[9] —, REFPROP 8.0,[24] $x_1 = 0.2500$ at (350 and 400) K; − − −, REFPROP 8.0,[24] $x_1 = 0.5158$ at (350 and 400) K; ···, REFPROP 8.0,[24] $x_1 = 0.8017$ at (350 and 400) K.

deviations near the dew point because the virial equation of state is best used to describe the $pvTx$ properties in the gaseous phase with densities lower than half of the critical density. The $pvTx$ properties from REFPROP 8.0[24] are compared to eq 7 at

Table 9. Experimental Second and Third Virial Coefficients for the CO_2 (1) + Propane (2) Mixtures from the Burnett Analysis

T/K	B_m/$cm^3\cdot mol^{-1}$	C_m/$cm^6\cdot mol^{-2}$
	$x_1 = 0.5158$	
320.008	−184.7	13378
330.010	−171.4	11746
340.011	−160.0	10862
350.011	−149.4	10037
360.012	−140.2	9629
370.020	−131.7	9203
380.027	−123.8	8846
390.030	−116.5	8510
400.033	−109.3	8074
	$x_1 = 0.8017$	
320.003	−128.9	6799
329.998	−120.1	6388
340.000	−112.0	5982
350.014	−104.9	5809
360.015	−98.2	5602
370.014	−91.8	5297
380.024	−86.1	5084
390.030	−80.6	4861
400.032	−76.3	4952

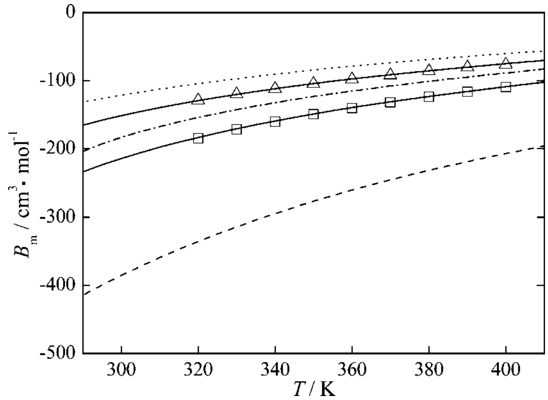

Figure 14. Temperature dependence of the second virial coefficients for CO_2 (1) + propane (2) mixtures: □, $x_1 = 0.5158$; △, $x_1 = 0.8017$; —, eq 10; —•—, B_{12} from eq 10; •••, the second virial coefficient of CO_2;[27] – – –, the second virial coefficient of propane.[21]

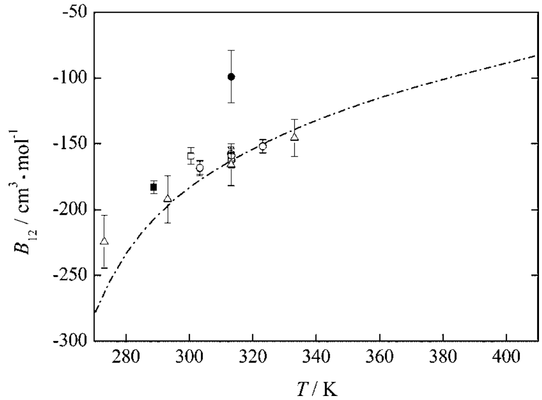

Figure 15. Second cross virial coefficients B_{12} for CO_2 (1) + propane (2) mixtures: —•—, eq 10; ■, Mason and Eakin;[10] ●, Sie et al.;[11] □, Bougard and Jadot;[12] ○, Michels et al.;[13] △, McElroy et al.[14]

$x_1 = 0.2500$, 0.5158, and 0.8017 in Figure 13. The maximum relative density deviation at 400 K is 0.4 % for $x_1 = 0.2500$ and 0.8017 with the discrepancies increasing as the temperature decreases. The difference between REFPROP 8.0[24] and eq 7 for $x_1 = 0.2500$ at 350 K reaches −2.4 % at 4400 kPa. The relative density deviations for mixture $x_1 = 0.5158$ are −1.0 % at 400 K and −1.5 % at 350 K.

The experimental second and third coefficients, $B_m(T)$ and $C_m(T)$, were obtained by directly fitting eq 7 to the experimental data along isotherms with the results listed in Table 9.

Table 10 and Figures 14 to 16 show the temperature dependence of the experimental and the values of B_m and C_m correlated using eqs 10 and 11 along with the virial coefficients of the pure components and cross virial coefficients of the CO_2 (1) + propane (2) mixture. The estimated uncertainties for a 95 % confidence level are ± 1 cm^3·mol^{-1} for B_m and ± 500 cm^6·mol^{-2} for C_m. The calculated second and third virial coefficients are both in good agreement with the experimental data after the careful measurements. The second cross virial coefficients from Mason and Eakin,[10] Sie et al.,[11] Bougard and Jadot,[12] Michels et al.,[13] and McElroy et al.[14] are also plotted in Figure 15. The second cross virial coefficients from eq 10 show good agreement with data from Michels et al.[13] and McElroy et al.[14] at temperatures from (293 to 333) K. The three data points from Mason and Eakin,[10] Sie et al.,[11] and Bougard and Jadot[12] show larger discrepancies than the others. The second cross virial coefficients from eq 10 at temperatures below 290 K are more negative than those from McElroy et al.[14] which may result in larger uncertainties of the extrapolated third virial coefficients at temperatures lower than 290 K.

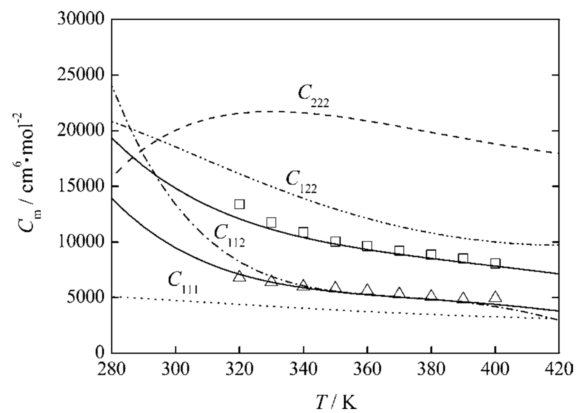

Figure 16. Temperature dependence of the third virial coefficients for CO_2 (1) + propane (2) mixtures: □, $x_1 = 0.5158$; △, $x_1 = 0.8017$; —, eq 11; •••, third virial coefficient of CO_2;[27] – – –, third virial coefficient of propane.[21]

Conclusions

The Burnett isochoric method was used to measure a total of 225 $pvTx$ data points in the gaseous phase for CO_2 + propane mixtures with CO_2 mole compositions of 0.5158 and 0.8017, temperatures from (320 to 400) K, and pressures up to 7784 kPa. The temperature and pressure measurement uncertainties were less than ± 5 mK and ± 300 Pa. Burnett measurements for pure helium, argon, and CO_2 were also conducted at 318 K and/or 343 K to validate the reliability of the experimental system and data reduction procedure. A truncated virial EOS was used to fit the experimental data with rms deviations of ± 0.03 %. The present virial equation of state compares well with

Table 10. Cross Second and Third Virial Coefficients Calculated from Virial Equations for CO_2 (1) + Propane (2) Mixtures

T/K	B_{11} / cm^3·mol^{-1}	B_{12} / cm^3·mol^{-1}	B_{22} / cm^3·mol^{-1}	C_{111} / cm^6·mol^{-2}	C_{112} / cm^6·mol^{-2}	C_{122} / cm^6·mol^{-2}	C_{222} / cm^6·mol^{-2}
320.000	−104.4	−154.0	−335.7	4388	8226	16123	21572
330.000	−97.1	−142.5	−314.3	4215	6892	14978	21722
340.000	−90.5	−132.3	−294.8	4050	6066	13917	21605
350.000	−84.4	−123.3	−277.0	3894	5572	12957	21301
360.000	−78.8	−115.2	−260.6	3748	5272	12112	20875
370.000	−73.6	−107.8	−245.6	3613	5060	11391	20377
380.000	−68.8	−101.1	−231.7	3489	4851	10796	19848
390.000	−64.4	−94.8	−218.9	3376	4581	10332	19318
400.000	−60.3	−88.7	−206.9	3274	4200	9997	18813

The second and third virial coefficients of pure CO_2 were calculated from Span and Wagner,[27] and those of propane were obtained from Lemmon et al.[21] by fitting the data from (220 to 450) K.

published $p\upsilon Tx$ data. The calculated virial coefficients B_m and C_m agree well with the experimental values.

Literature Cited

(1) Calm, J. M. The next generation of refrigerants - Historical review, considerations, and outlook. *Int. J. Refrig.* **2008**, *31*, 1123–1133.

(2) Niu, B. L.; Zhang, Y. F. Experimental study of the refrigeration cycle performance for the R744/R290 mixtures. *Int. J. Refrig.* **2007**, *30*, 37–42.

(3) Hegel, P. E.; Zabaloy, M. S.; Mabe, G. D. B.; Pereda, S.; Brignole, E. A. Phase equilibrium engineering of the extraction of oils from seeds using carbon dioxide plus propane solvent mixtures. *J. Supercrit. Fluids* **2007**, *42*, 318–324.

(4) Illes, V.; Szalai, O.; Then, M.; Daood, H.; Perneczki, S. Extraction of hiprose fruit by supercritical CO_2 and propane. *J. Supercrit. Fluids* **1997**, *10*, 209–218.

(5) Reamer, H. H.; Sage, B. H.; Lacey, W. N. Phase Equilibria in Hydrocarbon Systems - Volumetric and Phase Behavior of the Propane-Carbon Dioxide System. *Ind. Eng. Chem.* **1951**, *43*, 2515–2520.

(6) Niesen, V. G.; Rainwater, J. C. Critical Locus, (Vapor + Liquid) Equilibria, and Coexisting Densities of (Carbon Dioxide + Propane) at Temperatures from 311 K to 361 K. *J. Chem. Thermodyn.* **1990**, *22*, 777–795.

(7) Galicia Luna, L. A.; Richon, D.; Renon, H. New Loading Technique for a Vibrating Tube Densimeter and Measurements of Liquid Densities up to 39.5 MPa for Binary and Ternary Mixtures of the Carbon-Dioxide Methanol Propane System. *J. Chem. Eng. Data* **1994**, *39*, 424–431.

(8) de la Cruz de Dios, J.; Bouchot, C.; Galicia Luna, L. A. New *p-ρ-T* measurements up to 70 MPa for the system CO_2 plus propane between 298 and 343 K at near critical compositions. *Fluid Phase Equilib.* **2003**, *210*, 175–197.

(9) Blanco, S. T.; Gil, L.; Garcia-Gimenez, P.; Artal, M.; Otin, S.; Velasco, I. Critical Properties and High-Pressure Volumetric Behavior of the Carbon Dioxide plus Propane System at $T = 308.15$ K. Krichevskii Function and Related Thermodynamic Properties. *J. Phys. Chem. B* **2009**, *113*, 7243–7256.

(10) Mason, D. M.; Eakin, B. E. Compressibility Factor of Fuel Gases at 60 °F and 1 atm. *J. Chem. Eng. Data* **1961**, *6*, 499–504.

(11) Sie, T. T.; van Beersum, W.; Rijnders, G. W. High-Pressure Gas Chromatography and Chromatography with Supercritical Fluids. I. The Effect of Pressure on Partition Coefficients in Gas-Liquid Chromatography with Carbon Dioxide as a Carrier Gas. *Sep. Sci. Technol.* **1966**, *1*, 459–490.

(12) Bougard, J.; Jadot, R. 2nd Virial-Coefficient of Binary-Mixtures of Some Halocarbons. *J. Chim. Phys. Phys. Chim. Biol.* **1976**, *73*, 415–417.

(13) Michels, J. P. J.; Schouten, J. A.; Jaeschke, M. The Determination of the 2nd and 3rd Virial-Coefficients from *Pvt-X* Data of Binary-Systems. *Int. J. Thermophys.* **1988**, *9*, 985–992.

(14) McElroy, P. J.; Lim, L. K.; Renner, C. A. Excess 2nd Virial Coefficients for Binary Mixtures of Carbon Dioxide with Methane, Ethane, and Propane. *J. Chem. Eng. Data* **1990**, *35*, 314–317.

(15) Dymond, J. H.; Mash, K. N.; Wilhoit, R. C. *Virial Coefficients of Pure Gases and Mixtures*, Vol. 21; Springer: New York, 2002.

(16) Feng, X. J.; Xu, X. H.; Fang, J.; Lin, H.; Duan, Y. Y. Precise measurement system for thermophysical properties of fluids. *J. Eng. Thermophys.* **2009**, *30*, 565–568.

(17) Feng, X. J.; Xu, X. H.; Lin, H.; Duan, Y. Y. Vapor pressures of 1,1,1,2,3,3,3-heptafluoropropane, 1,1,1,3,3,3-hexafluoropropane and 1,1,1,3,3-pentafluoropropane. *Fluid Phase Equilib.* **2010**, *290*, 127–136.

(18) Lemmon, E. W.; Goodwin, A. R. H. Critical properties and vapor pressure equation for alkanes C_nH_{2n+2}: Normal alkanes with $n \leq 36$ and isomers for $n = 4$ through $n = 9$. *J. Phys. Chem. Ref. Data* **2000**, *29*, 1–39.

(19) McLinden, M. O. Thermodynamic Properties of Propane. I. *p-ρ-T* Behavior from (265 to 500) K with Pressures to 36 MPa. *J. Chem. Eng. Data* **2009**, *54*, 3181–3191.

(20) Thomas, R. H. P.; Harrison, R. H. Pressure-Volume-Temperature Relations of Propane. *J. Chem. Eng. Data* **1982**, *27*, 1–11.

(21) Lemmon, E. W.; McLinden, M. O.; Wagner, W. Thermodynamic Properties of Propane. III. A Reference Equation of State for Temperatures from the Melting Line to 650 K and Pressures up to 1000 MPa. *J. Chem. Eng. Data* **2009**, *54*, 3141–3180.

(22) Kratzke, H. Thermodynamic Quantities for Propane 0.1. the Vapor-Pressure of Liquid Propane. *J. Chem. Thermodyn.* **1980**, *12*, 305–309.

(23) Burnett, E. S. *Application of the Burnett Method of Compressibility Determinations to Multiphase Fluid Mixtures*; Bureau of Mines: Washington, DC, 1963.

(24) Lemmon, E. W.; McLinden, M. O.; Meier, K. *Reference Fluid Thermodynamic and Transport Properties (REFPROP)*, NSRD; NIST: Gaithersburg, MD, 2007.

(25) Feng, X. J.; Duan, Y. Y. Random and Systematic Errors Propagation in *pυTx* Properties Measurements with Burnett-Isochoric Method, in 17th Symposium on Thermophysical Properties, Boulder, CO, 2009.

(26) Gupta, D.; Eubank, P. T. Density and Virial Coefficients of Gasesous Butane from 265 to 450 K at Pressures to 3.3 MPa. *J. Chem. Eng. Data* **1997**, *42*, 961–970.

(27) Span, R.; Wagner, W. A new equation of state for carbon dioxide covering the fluid region from the triple-point temperature to 1100 K at pressures up to 800 MPa. *J. Phys. Chem. Ref. Data* **1996**, *25*, 1509–1596.

(28) Tegeler, C.; Span, R.; Wagner, W. A new equation of state for argon covering the fluid region for temperatures from the melting line to 700 K at pressures up to 1000 MPa. *J. Phys. Chem. Ref. Data* **1999**, *28*, 779–850.

(29) Duschek, W.; Kleinrahm, R.; Wagner, W. Measurement and Correlation of the (Pressure, Density, Temperature) Relation of Carbon Dioxide 0.2. Saturated-Liquid and Saturated-Vapor Densities and the Vapor-Pressure Along the Entire Coexistence Curve. *J. Chem. Thermodyn.* **1990**, *22*, 841–864.

Received for review February 9, 2010. Accepted June 2, 2010. This work was supported by the National Natural Science Foundation of China (No. 50636020) and the National Key Technology R&D Program (2006BAF06B03).

JE100148H